PNAS
www.pnas.org

Supplementary Information for

Computational and Experimental Insights into the Circadian Effects of SIRT1

Panagiota T. Foteinou, Anand Venkataraman, Lauren J. Francey, Ron C. Anafi, John B. Hogenesch and Francis J. Doyle III
Francis J. Doyle III
Email: frank_doyle@seas.harvard.edu

This PDF file includes:

Supplementary text
Figs. S1 to S9
Tables S1 to S7
References for SI reference citations

Supplemental Experimental Procedures

siRNA transfections and kinetic bioluminescence recording. Cells were transfected using Lipofectamine RNAiMAX transfection reagent (Invitrogen) with 12pmol siRNA against all genes except *BMAL1*. Only 3pmol of the siRNA against *BMAL1* was transfected to prevent complete arrhythmicity. A negative control siRNA (AllStars Negative control siRNA; Qiagen) was used to ensure equal molar amounts of siRNA in all reactions. Two days post transfection, the cell-culture medium was changed to a recording medium [made up of phenol-red free DMEM (Sigma, D-2902), 4mM sodium bicarbonate (Sigma, S5761), 10mM HEPES buffer (Gibco, 15630-122), 1x PSG, 0.1mM luciferin (Promega) and 0.1µM Dexamethasone (Sigma)] and the plates were sealed shut using their own lids with sterile vacuum grease. Sealed plates were then placed into a LumiCycle luminometer (Actimetrics) and luminescence was measured for over 5 days. Alternatively, a linearly scaled down version of the above mentioned protocol was also used to record luminescence in a 96 well plate format using the Synergy2 BioTek microplate reader.

Calculation of period length, amplitude and baseline. Circadian period from the luminescence recordings was calculated using the WAVECLOCK package (1) on a Dell desktop PC running R for Windows version 2.7.0 (http://www.R-project.org) This wavelet-based assessment of period varies as a function of time and the median period, corresponding to the "total mode", was used to describe the overall period. Waveforms with dominant non-circadian periods (outside the range of 20 – 28 hours) were considered arrhythmic. Circadian amplitude was determined by regression to a sinusoidal waveform with the previously established period using the lm() function in R. Baseline estimates used are the mean of all luminescence values recorded between day 1 and day 4 of the experiment.

Isolation of RNA and gene expression assays. Reverse transcription of 0.5-1 µg of RNA was performed using qScript™ cDNA Synthesis Kit (Quanta Biosciences) and quantitative RT-PCR was performed using TaqMan gene expression assays (Applied Biosystems and IDT) and PerfeCTa® FastMix® II (Quanta Biosciences) as per the manufacturer's instructions. Catalog numbers of the primers used in this manuscript are listed in **Table S3**.

Model derivation for the SIRT1-dependent deacetylation of BMAL1 and PER2 (model A). The following assumptions were made for the development of this model:

i. In agreement with experimental observations (2), the canonical transcriptional/translational (PER-CRY/CLOCK-BMAL1) feedback loop is considered to be the primary generator of circadian oscillations. Complementary to this, the rhythmic regulation of the positive element, *BMAL1* transcription, by a second transcriptional feedback loop that involves the nuclear receptors REV-ERB and ROR, is not required for the generation of endogenous oscillations (3). Consequently, we assume constitutive expression of *BMAL1* gene expression.

ii. For the purpose of simplicity, the mammalian homologs of period (*PER1*, *PER2* and *PER3*) and cryptochrome (*CRY1*, *CRY2*) genes are not explicitly modeled. Instead, they are represented by combined variables (*PER* and *CRY*) both at the mRNA and protein level.

iii. At the mRNA level, SIRT1 is produced almost at constant levels (4) (similar to the constitutive levels of *CLOCK* expression in most tissues (5, 6)) and thereby both *CLOCK* and *SIRT1* dynamics are not described by explicit model variables. Instead, the model assumes NAD^+ levels represent SIRT1 deacetylase activity, whose oscillations are in phase. In the case of the constitutive *CLOCK* expression, the concentration of the nuclear CLOCK-BMAL1 complex is represented by the nuclear (active) BMAL1 and therefore such terms are used interchangeably.

iv. Although core loop components have many post-translational modifications, this study focuses on the role of acetylation in the circadian function (7). Of particular interest is how SIRT1 deacetylates nuclear BMAL1 and PER.

v. Since SIRT1-mediated deacetylation promotes proteasomal degradation, the acetylated levels of nuclear proteins BMAL1 and PER represent the active entities. The PER-CRY complex is assumed to exist either in the acetylated (active) form or non-acetylated (inactive). Similarly, BMAL1 levels are considered as acetylated (active) BMAL1 and non-acetylated (inactive).

The mathematical formulation of model A, which is illustrated in **Fig. 1*A***, consists of thirteen (13) ordinary differential equations (ODEs) and fifty-six (56) kinetic parameters. These state variables represent the kinetics of mRNA abundance of *PER* (M_{PER}), *CRY* (M_{CRY}) and *NAMPT* (M_{NAMPT}) genes, as well as the corresponding protein concentrations in the cytosol (PER, CRY, NAMPT). Cytoplasmic and nuclear PER-CRY heterodimers are represented by PCC and PCN, respectively. The variable NAD describes cellular levels of NAD^+. Cytosolic and nuclear concentrations of BMAL1 protein are denoted by BC and BN. Further, the acetylated forms of the activator BMAL1 and the repressor complex PER-CRY are represented by BN_{ac} and PCN_{ac}, respectively. The model dynamics are described by the following system of ODEs (S1.1) – (S1.4):

(a) mRNA dynamics of E-box genes (*PER, CRY* and *NAMPT*)

$$\frac{dM_i}{dt} = v_{0i} + \frac{v_{si}\cdot BN_{ac}^{a}}{K_{A_i}^{a}\cdot\left(1+\left(\frac{PCN_{ac}}{R_i}\right)^{r}\right)+BN_{ac}^{a}} - \frac{v_{di}\cdot M_i}{K_{di}+M_i} - k_{dn}\cdot M_i, \quad i = \{PER,\ CRY,\ NAMPT\} \tag{S1.1}$$

(b) cytosolic proteins/complexes

$$\begin{aligned}
\frac{dPER}{dt} &= k_{sP}\cdot M_{Per} + k_{d,PC}\cdot PCC - k_{a,PC}\cdot PER\cdot CRY - \frac{v_{dP}\cdot PER}{K_{dp}+PER} - k_{dn}\cdot PER \\
\frac{dCRY}{dt} &= k_{sC}\cdot M_{Cry} + k_{d,PC}\cdot PCC - k_{a,PC}\cdot PER\cdot CRY - \frac{v_{dC}\cdot CRY}{K_{dc}+CRY} - k_{dn}\cdot CRY \\
\frac{dPCC}{dt} &= k_{a,PC}\cdot PER\cdot CRY - k_{d,PC}\cdot PCC - k_{im,PC}\cdot PCC + k_{ex,PC}\cdot PCN - \frac{v_{dPCC}\cdot PCC}{K_{dPCC}+PCC} - k_{dn}\cdot PC_c \\
\frac{dBC}{dt} &= k_{sB} - k_{im,B}\cdot BC + k_{ex,B}\cdot BN - \frac{v_{dBc}\cdot BC}{K_{dBc}+BC} - k_{dn}\cdot BC
\end{aligned} \tag{S1.2}$$

(c) nuclear proteins/complexes

$$
\begin{aligned}
\frac{dPCN}{dt} &= k_{im,PC}\cdot PCC - k_{ex,PC}\cdot PCN - \frac{v_{PAC}\cdot PC_N}{K_{PAC}+PC_N} + \frac{v_{PDAC}\cdot NAD\cdot PCN_{ac}}{K_{PDAC}+PCN_{ac}} - \frac{v_{dPCN}\cdot PCN}{K_{dPCN}+PCN} - k_{dn}\cdot PCN \\
\frac{dPCN_{ac}}{dt} &= \frac{v_{PAC}\cdot PC_N}{K_{PAC}+PC_N} - \frac{v_{PDAC}\cdot NAD\cdot PCN_{ac}}{K_{PDAC}+PCN_{ac}} - k_{dn}\cdot PCN_{ac} \\
\frac{dBN}{dt} &= k_{im,B}\cdot BC - k_{ex,BC}\cdot BN - \frac{v_{BAC}\cdot BN}{K_{BAC}+BN} + \frac{v_{BDAC}\cdot NAD\cdot BN_{ac}}{K_{BDAC}+B_{Nac}} - \frac{v_{dBN}\cdot BN}{K_{dBN}+BN} - k_{dn}\cdot BN \\
\frac{dBN_{ac}}{dt} &= \frac{v_{BAC}\cdot BN}{K_{BAC}+BN} - \frac{v_{BDAC}\cdot NAD\cdot BN_{ac}}{K_{BDAC}+B_{Nac}} - k_{dn}\cdot BN_{ac}
\end{aligned}
\qquad \text{(S1.3)}
$$

(d) NAMPT/NAD loop

$$
\begin{aligned}
\frac{dNAMPT}{dt} &= k_{sN}\cdot M_{Nampt} - \frac{v_{dN}\cdot NAMPT}{K_{dN}+NAMPT} - k_{dn}\cdot NAMPT \\
\frac{dNAD}{dt} &= s_n\cdot NAMPT - \frac{v_{dNAD}\cdot NAD}{K_{dNAD}+NAD} - k_{dn}\cdot NAD
\end{aligned}
\qquad \text{(S1.4)}
$$

As shown above, transcription is mathematically described by Hill equations (an expression commonly used in the literature (8, 9) characterized by five parameters representing the maximum velocity v_{si} (i = *PER*, *CRY*, *NAMPT*), two DNA binding constants of an activator (K_{Ai}) and a repressor (R_i, i = Per, Cry, Nampt) and two Hill coefficients for activation (a) and repression (r). We further introduced basal synthesis rate for v_{0i} (i = *PER*, *CRY*, *NAMPT*), which represents transcriptional activation from the constitutive promoter. Translation rate is proportional to mRNA concentration with the kinetic constant (k_{si}, i = P, C, N). The law of mass action describes association and dissociation of PER-CRY complexes, nuclear transportation, and reversible acetylations. Michaelis-Menten-type equations are employed to describe enzyme-mediated degradation processes. Nonspecific degradation terms are also incorporated and are proportional to each variable with the kinetic constant k_{dn}. Taken together, this model integrates the classical PER-CRY transcriptional feedback loop with the circadian NAMPT/NAD^+ enzymatic loop.

Equation (S1). Let us consider an ordinary differential equation system (ODE)

$$\frac{d\mathbf{x}}{dt} = F(\mathbf{x},\mathbf{p}), \quad \mathbf{x}\in\mathbb{R}^n,\ \mathbf{p}\in\mathbb{R}^m$$

where **x** denotes the vector of state variables and **p** the vector of parameters. Suppose that this system has a stable periodic solution with period (T). Using the scaling

$$\tau_0 = \frac{t}{T}$$

the system reads as follows:

$$\frac{d\mathbf{x}}{d\tau_0} = TF(\mathbf{x},\mathbf{p}), \quad \mathbf{x}\in\mathbb{R}^n,\ \mathbf{p}\in\mathbb{R}^m$$

with $\tau_0 \in (0,1)$. In order for the system to yield a period close to naturally occurring in continuous darkness (τ_{dd}), the system is transformed as

$$\frac{d\mathbf{x}}{d\tau} = \frac{T}{\tau_{dd}} F(\mathbf{x}, \mathbf{p}), \quad \mathbf{x} \in \mathbb{R}^n, \ \mathbf{p} \in \mathbb{R}^m$$

with $\tau \in (0, \tau_{dd})$; hence all rate parameters are multiplied by the scaling factor (T/τ_{dd}). In this study the cell autonomous period (τ_{dd}) is considered to be 23.7h which is the average period of an individual circadian oscillator (23.7 ± 1.2 h) (10).

Self-sustained oscillations and relevant phases. We tested the ability of our proposed circadian oscillator model to reproduce experimentally observed sustained oscillations. Using the parameter values as shown in **Table S1** our first modeling effort (model A) can reproduce cell autonomous oscillations with relevant phase relations as illustrated in **Table S5**. Specifically, for both parameter sets (H1 and H2) the mRNA of co-regulated E-box genes (PER, CRY, NAMPT) peaks early during the subjective night while the circadian levels of the protein NAMPT and NAD cofactor peak later in the middle of the subjective night. Such phase delay is related to the upregulation of metabolic processes during the fasting period. Further, the model reproduces a 4-hour phase relationship between PER mRNA and PER protein, which lies within the experimental range of a 4-hour to 8-hour delay (5). In this model, the rhythmic levels of PER, rather than CRY, are critical for circadian oscillations which are consistent with experimental findings from these studies (11, 12). Meanwhile the simulated circadian oscillations of acetylated BMAL1 ($BMAL1^{AC}$) are almost antiphasic to the variation levels of NAD regulator. Importantly, Nakahata et al. (4) found in both synchronized fibroblasts and liver tissue that the peak phase of SIRT1 deacetylase activity is consistent with the low levels of cyclic acetylation of histone H3 and non-histone substrates (i.e. BMAL1). In regard to phase relation between SIRT1 (or NAD) activity and acetylated PER (PER^{AC}-CRY), it is noteworthy that the model predicts an in-phase relationship. This is captured for parameter set H2 where SIRT1 regulates the dynamics of PER^{AC}-CRY (negative clock component). As the active repressor, PER^{AC}-CRY is expected to peak late in the evening, which is experimentally shown in (13) and also reproduced by the model. For the parameter set H1, an in-phase relationship between the peak phases of SIRT1 and PER^{AC}-CRY is not necessary. This explains the phase difference (advance) simulated for NAD when parameter set H1 is compared with set H2 (**Table S5**).

Model derivation for the SIRT1-dependent regulation of PGC1α, BMAL1 and PER2 (model B). The following assumptions were made for the development of this model:

i. All members of the ROR (α, β and γ) and REV-ERB subfamilies (α and β) are not explicitly modeled. Instead, they are represented by combined variables (ROR and REV-ERB) both at the mRNA and protein level.
ii. At the mRNA level, the transcription of *ROR* genes is assumed to be regulated not only by the core PER/CRY loop (E-box regulation) but also directly by the ROR/REV-ERB loop (RORE mediated regulation). This assumption is in agreement with the experimental findings of Liu et al. (3), which indicate that *ROR* harbors a functional RORE.
iii. For the sake of simplicity, the model does not distinguish between rhythmic *PGC1α* expression and the corresponding protein. Instead, the variable PGC1α is assumed to represent the rhythmic activity of PGC1α that depends upon NAD^+-dependent deacetylation by SIRT1. Quantitatively, the induction of PGC1α by SIRT1 is described by a Michaelis-Menten type equation while a basal rate and non-specific degradation term are used to describe constitutive activation.
iv. The stimulatory activity of the protein ROR at the ROR-binding sites (RORE) is exerted via its synergistic action with the transcriptional coactivator PGC1α (14), a transcriptional regulator highly responsive to nutrient signals. This interaction results in the formation of the complex (ROR^*) which represents the active ROR protein.
v. With regard to the core PER/CRY loop, the model distinguishes two homologs of the PER subfamily (*PER1* and *PER2* genes) and SIRT1 regulates the acetylation level of PER2. The sum of the PER1/CRY complex and the active (acetylated) PER2/CRY (denoted P1C and $P2C_{ac}$, respectively) represent the total (active) PER/CRY repressor.
vi. For the purpose of simplicity, we only consider reversible entry of the cytosolic protein BMAL1 into the nucleus (denoted BC and BN, respectively). Nuclear BMAL1 undergoes reversible acetylation regulated by SIRT1, consistent with model A.

The model described in this section explicitly considers the rhythmic regulation of *BMAL1* transcription by the auxiliary ROR/REV-ERB feedback loop (model B). Within this loop, the clock genes *ROR* (M_{ROR}) and *NR1D1*/2 (M_{REV}) are transcribed and translated into the corresponding proteins ROR and REV-ERB (REV), which regulate *BMAL1* expression (M_B) by competing at the BMAL1 promoter as activator and repressor, respectively. The dynamics of this model illustrated in **Fig. 2** are described by the following system of ODEs (S1.5) – (S1.9):

(a) mRNA dynamics of E-box and RORE genes

$$\frac{dM_i}{dt} = v_{0i} + \frac{v_{si}\cdot BN_{ac}^{a}}{K_{A_i}^{a}\cdot\left(1+\left(\frac{P1C}{R_i}+\frac{P2C_{ac}}{R_i^{'}}\right)^{r}\right)+BN_{ac}^{a}} - \frac{v_{di}\cdot M_i}{K_{di}+M_i} - k_{dn}\cdot M_i, \qquad \text{(S1.5)}$$

$$i = \{PER1,\ \ PER2,\ \ CRY,\ \ REV,\ \ NAMPT\}$$

$$\frac{dM_B}{dt} = v_{0B} + \frac{v_{sB}\cdot ROR^{*b}}{K_{AB}^{b}\left(1+\left(\frac{REV}{R_B}\right)^{c}\right)+ROR^{*b}} - \frac{v_{dB}\cdot M_B}{K_{dB}+M_B} - k_{dn}\cdot M_B$$

$$\frac{dM_{Ror}}{dt} = v_{0Ror} + \frac{v_{s1Ror}\cdot BN_{ac}^{a}}{K_{A1ror}^{a}\cdot\left(1+\left(\frac{P1C}{R_{1Ror}}+\frac{P2C_{ac}}{R_{1Ror}^{'}}\right)^{r}\right)+BN_{ac}^{a}} + \frac{v_{s2Ror}\cdot ROR^{*b}}{K_{A2ror}^{b}\left(1+\left(\frac{REV}{R_{2Ror}}\right)^{c}\right)+ROR^{*b}} - \frac{v_{dRor}\cdot M_{Ror}}{K_{dRor}+M_{Ror}} - k_{dn}\cdot M_{Ror} \qquad \text{(S1.6)}$$

(b) Proteins/complexes of PER1/CRY loop

$$\frac{dPER1}{dt} = k_{sP}\cdot M_{Per1} + k_{d,P1C}\cdot P1C - k_{a,P1C}\cdot PER1\cdot CRY - \frac{v_{dP1}\cdot PER1}{K_{dp}+PER1} - k_{dn}\cdot PER1$$

$$\frac{dCRY}{dt} = k_{sC}\cdot M_{Cry} + k_{d,P1C}\cdot P1C - k_{a,P1C}\cdot PER1\cdot CRY - \frac{v_{dC}\cdot CRY}{K_{dc}+CRY} - k_{dn}\cdot CRY$$

$$\frac{dP1C}{dt} = k_{a,P1C}\cdot PER1\cdot CRY - k_{d,P1C}\cdot P1C - \frac{v_{dP1C}\cdot P1C}{K_{dP1C}+P1C} - k_{dn}\cdot P1C$$

(c) Proteins/complexes of PER2/CRY loop

$$
\begin{aligned}
\frac{dPER2}{dt} &= k_{sP}\cdot M_{Per1} + k_{d,P2C}\cdot P2C - k_{a,P2C}\cdot PER2\cdot CRY - \frac{v_{dP2}\cdot PER2}{K_{dP}+PER2} - k_{dn}\cdot PER2 \\
\frac{dCRY}{dt} &= k_{sC}\cdot M_{Cry} + k_{d,P1C}\cdot P1C - k_{a,P1C}\cdot PER1\cdot CRY + k_{d,P2C}\cdot P2C - k_{a,P2C}\cdot PER2\cdot CRY \\
&\quad - \frac{v_{dC}\cdot CRY}{K_{dc}+CRY} - k_{dn}\cdot CRY \\
\frac{dP2C}{dt} &= k_{a,P2C}\cdot PER2\cdot CRY - k_{d,P2C}\cdot P2C - \frac{v_{PAC}\cdot P2C}{K_{PAC}+P2C} + \frac{v_{PDAC}\cdot NAD\cdot P2C_{ac}}{K_{PDAC}+P2C_{ac}} \\
&\quad - \frac{v_{dP1C}\cdot P2C}{K_{dP1C}+P2C} - k_{dn}\cdot P2C \\
\frac{dP2C_{ac}}{dt} &= \frac{v_{PAC}\cdot P2C}{K_{PAC}+P2C} - \frac{v_{PDAC}\cdot NAD\cdot P2C_{ac}}{K_{PDAC}+P2C_{ac}} - k_{dn}\cdot P2C_{ac}
\end{aligned}
\qquad \text{(S1.6)}
$$

(d) Cytosolic/nuclear BMAL1

$$
\begin{aligned}
\frac{dBC}{dt} &= k_{sB}\cdot M_B - k_{im,B}\cdot BC + k_{ex,B}\cdot BN - \frac{v_{dBc}\cdot BC}{K_{dBc}+BC} - k_{dn}\cdot BC \\
\frac{dBN}{dt} &= k_{im,B}\cdot BC - k_{ex,BC}\cdot BN - \frac{v_{BAC}\cdot BN}{K_{BAC}+BN} + \frac{v_{BDAC}\cdot NAD\cdot BN_{ac}}{K_{BDAC}+B_{Nac}} - \frac{v_{dBN}\cdot BN}{K_{dBN}+BN} - k_{dn}\cdot BN \\
\frac{dBN_{ac}}{dt} &= \frac{v_{BAC}\cdot BN}{K_{BAC}+BN} - \frac{v_{BDAC}\cdot NAD\cdot BN_{ac}}{K_{BDAC}+B_{Nac}} - k_{dn}\cdot BN_{ac}
\end{aligned}
\qquad \text{(S1.7)}
$$

(e) Proteins/complexes of ROR/REV-ERB loop

$$
\begin{aligned}
\frac{dREV}{dt} &= k_{sREV}\cdot M_{Rev} - \frac{v_{dREV}\cdot REV}{K_{dREV}+REV} - k_{dn}\cdot REV \\
\frac{dROR}{dt} &= k_{sROR}\cdot M_{Ror} - \frac{v_{dROR}\cdot ROR}{K_{dROR}+ROR} - k_{a,RP}\cdot PGC1\alpha\cdot ROR + k_{d,RP}\cdot ROR^{*} - k_{dn}\cdot ROR \\
\frac{dPGC1\alpha}{dt} &= v_{0pgc} + \frac{v_{spgc}\cdot NAD}{K_{Apgc}+NAD} - k_{a,RP}\cdot PGC1\alpha\cdot ROR + k_{d,RP}\cdot ROR^{*} \\
&\quad - \frac{v_{dpgc}\cdot PGC1\alpha}{K_{dpgc}+PGC1\alpha} - k_{dn}\cdot PGC1\alpha \\
\frac{dROR^{*}}{dt} &= k_{a,RP}\cdot ROR\cdot PGC1\alpha - k_{d,RP}\cdot ROR^{*}
\end{aligned}
\qquad \text{(S1.8)}
$$

(f) NAMPT/NAD loop

$$
\begin{aligned}
\frac{dNAMPT}{dt} &= k_{sN}\cdot M_{Nampt} - \frac{v_{dN}\cdot NAMPT}{K_{dN}+NAMPT} - k_{dn}\cdot NAMPT \\
\frac{dNAD}{dt} &= s_n\cdot NAMPT - \frac{v_{dNAD}\cdot NAD}{K_{dNAD}+NAD} - k_{dn}\cdot NAD
\end{aligned}
\qquad \text{(S1.9)}
$$

As shown in equations (S1.5) – (S1.9) this mathematical model is characterized by 19 ODEs and 92 kinetic parameters, which are estimated using the same evolutionary search algorithm as previously described . Additional constraints set by relevant experimental observations are

considered in the cost function and summarized in **Table S4**. Among these, a major constraint is related to the dominant effects of REV-ERB within the ROR/REV-ERB loop. Specifically, the model should allow the simulation of increased baseline of *BMAL1* oscillations in the loss-of-function mutation for *BMAL1* as we have previously shown in the study (15). Further data are related to the downregulatory effects of *SIRT1* null mutation (*SIRT1*$^{-/-}$) on *BMAL1* expression as previously shown (13). The proposed model is calibrated using published data and validated using additional RNA interference technology (RNAi) knockdown experiments.

Estimation of model parameters. To estimate the unknown parameters, an evolutionary algorithm was performed minimizing a particular cost function using the MATLAB Distributed Computing Toolbox. The cost function is defined as the discrepancy (*error*) between the output of the model and the data that comes from experiments. Experimental data (i.e. phases) from canonical clock genes and metabolites (4, 6, 16-20) were used. Appropriate parameters are chosen as those that satisfy these criteria (also in **Table S4**): (i) self-sustained oscillations are due to PER-CRY negative feedback loop; (ii) *SIRT1* loss does not result in arrhythmicity (in this model, *SIRT1*$^{-/-}$ is equivalent to NAD$^{-/-}$); (iii) simulation of either increased or decreased amplitude due to lack of enzymatic (NAD) activity as shown by Nakahata et al. (4) and Asher et al. (13), respectively. This estimation algorithm allows therefore for the generation of two independent parameter sets (referred to here as sets H1 and H2). Set H1 refers to the parameters for which the model simulates increased amplitude phenotype in response to lack of *SIRT1* (*SIRT1*$^{-/-}$), while set H2 refers to the parameters used in the model to simulate reduced amplitude response. To generate these two parameter sets, we used an "unsupervised" parameter estimation algorithm that utilizes a diverse set of experimental data to calibrate the model; without supervising for the identification of a few parameter combinations that dictate model behavior across the two paradoxical *SIRT1*$^{-/-}$ phenotypes. Given the prevalence of sloppiness – an apparently universal property of systems biology models (21) – many parameters are expected to vary across the two sets H1 and H2. Briefly, sloppiness suggests that collective fits to even large amounts of ideal (experimental) data often leave many parameters poorly constrained. Consequently, the model behavior depends on only a few ("stiff") parameter combinations. Further, the prevalence of sloppiness highlights the power of collective fits and suggests focusing on predictions rather than on parameters. Although a "supervised" approach could plausibly identify fewer more critical parameter combinations, we believe that either approach would ultimately yield similar predictions. Once a certain range of parameter values is captured for which the model produces periodic solutions and relevant phases, its period is scaled using **Equation S1** (see supplemental experimental procedures) so as to yield a typical period of an individual (circadian) oscillator close to 24h (i.e. 23.7h) (22, 23).

Design of *in silico* knockdown experiments. The performance of the extended circadian-enzymatic model (model B) is assessed through its ability to predict experimentally observed phenotypes of various genetic perturbations of circadian clock components. We have devised three levels of *in silico* predictions that are consistent with the RNAi validation experiments including: (i) circadian effects of *SIRT1* knockdown on circadian oscillations following *BMAL1* knockdown; (ii) circadian effects of *SIRT1* knockdown when expression of *CLOCK* is inhibited, and (iii) circadian effects of *SIRT1* knockdown when *PER2, PGC1α* or *ROR* is knocked down. In order to simulate the effect of a knockdown experiment, the effect of interference could be simulated either at the RNA level by increasing the RNA degradation rate or at the protein level by reducing the translation rate. Both methods give similar results except for the *BMAL1* knockdown experiment. Increasing the RNA degradation rate of *BMAL1* enables the model to robustly predict reduced *BMAL1* expression, consistent with the experimentally observed reduction of endogenous mRNA. Reducing the translation rate enables the model to simulate increased baseline of *BMAL1* mRNA. While this is consistent with the effect of *BMAL1* knockdown on *BMAL1* luciferase oscillations, it does not correlate with the cognate mRNA. We

simulated *BMAL1* knockdown by reducing the translation rate since the measured *BMAL1* luciferase oscillations represent the output of the *BMAL1* promoter (mathematically described by the variable M_B). Reducing the kinetic parameters of acetylation (v_{BAC}) and synthesis rate (s_n) of BMAL1 and NAD respectively simulates the effect of *CLOCK* and *SIRT1* knockdown. Note that both *CLOCK* and *SIRT1* are implicitly considered in this model (constitutive expression) and therefore their knockdowns could not be tested *in silico* at the RNA level.

Supplemental Figures

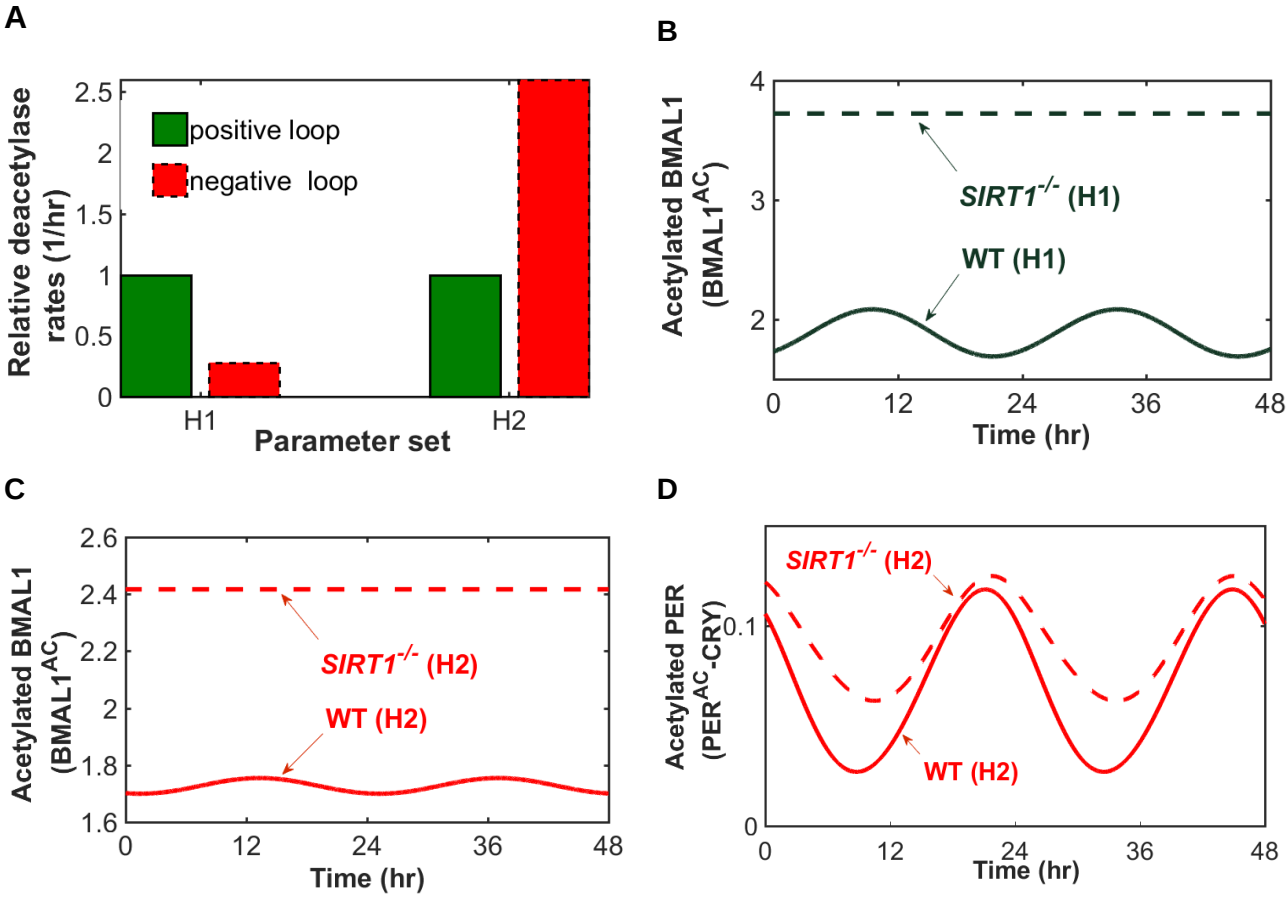

Fig. S1. Related to Figure 1. (A) Deacetylase rates in the negative loop relative to the positive loop. When H1 mechanism prevails, the rate of SIRT1 deacetylase in the negative loop (v_{PDAC}/K_{PDAC}) is much smaller than in the positive loop (v_{BDAC}/K_{BDAC}) while the opposite occurs when H2 mechanism dominates. For each parameter set (H1 and H2) the deacetylase rates are relative to the rate in the positive loop. **(B, C)** Rhythmic versus constitutive acetylation of BMAL1. Solid lines represent the wildtype (WT) dynamics of acetylated BMAL1 ($BMAL1^{AC}$) simulated using the parameter values of Table S1 (set H1). Dashed lines correspond to the *SIRT1* null mutant (*SIRT1*$^{-/-}$). **(D)** Dynamics of acetylated repressor (PER^{AC}-CRY) under control wildtype (WT) and *SIRT1*$^{-/-}$ conditions. The model simulates elevated acetylation levels of PER protein in the *SIRT1*$^{-/-}$ mutant as reported by Asher et al (13) using the H2 parameter set.

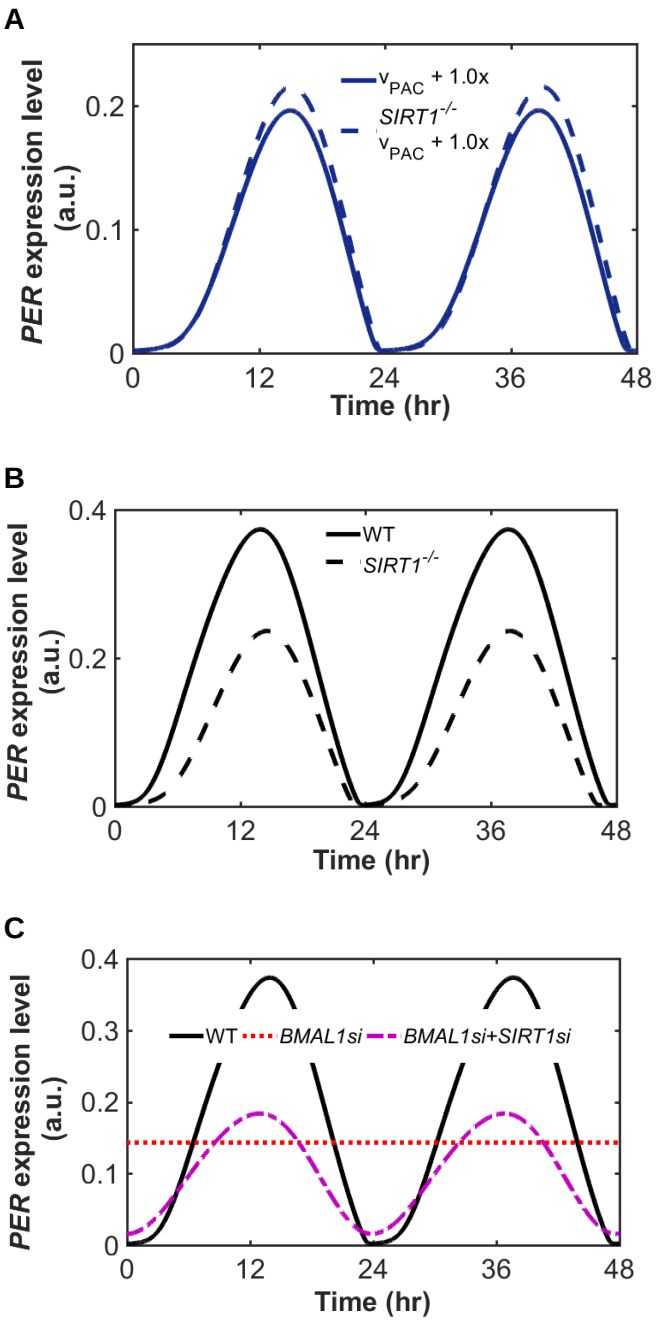

Fig. S2. Related to Figure 1. (A, B) Variation in the acetylation rate of repressor leads to dynamic changes in the amplitude response due to lack of *SIRT1*. Solid lines represent wildtype (WT) dynamics simulated using parameter set H2, while dashed line is simulated using the same parameter values except for the parameter v_{PAC} which is increased by 100% (v_{PAC} + 1.0x). Under this single parametric perturbation, the amplitude in the absence of SIRT1 switches from a reduction (black dashed line, B panel) to an increase (blue dashed line, A panel). **(C)** Variations of the strength of the positive and enzymatic feedback lead to a rescue of arrhythmicity. Simulated loss of oscillations (red dotted line) caused by a variation of the positive feedback (*BMAL1si*) are rescued by loss-of-function mutation for SIRT1 (magenta dashed line). The positive feedback is varied by a 55% decrease in the synthesis rate of BMAL1 activator while the synthesis rate (s_n) of NAD which in this model represents SIRT1 is reduced by 50%. Black solid line represent control wildtype (WT) dynamics of *PER* expression simulated using parameter set H2. Similar responses

277 are also simulated using parameter set H1. For reasons of clarity, the simulated *PER* expression in response
278 to *SIRT1si* is omitted (similar to the dynamics illustrated in Figure 1*B*).

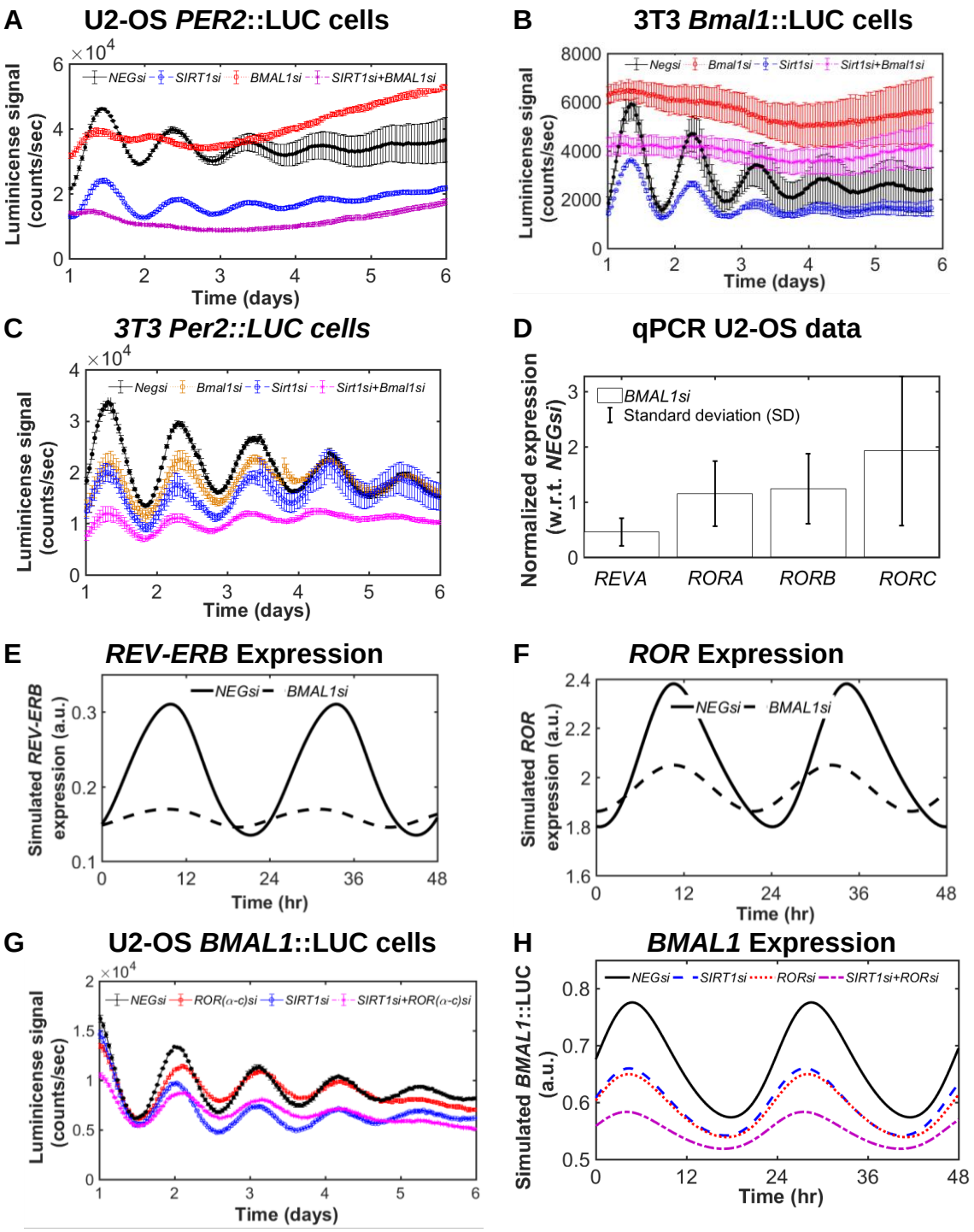

Fig. S3. Related to Figure 2. (**A**) Luciferase counts measured in U2-OS *PER2*::LUC cells transfected with siRNAs targeting *BMAL1*, *SIRT1* or both. (**B, C**) Luciferase counts measured in 3T3 *Bmal1*:LUC and *Per2*::LUC cell-lines respectively, following transfections with siRNAs targeting *Sirt1*, *Bmal1* or both. Data are represented as mean ± SEM. **(D)** Experimentally measured mRNA expression levels of *NR1D1* (*REVA*) and all three isoforms of *ROR* under *BMAL1si* condition normalized to control (*NEGsi*). Data are represented as mean ± SD. **(E, F)** Simulated expression levels of *REV-ERB* and *ROR* under control (solid lines) and *BMAL1si* conditions (dashed lines) while considering that SIRT1 can deacetylate PER2, BMAL1 and PGC1α. **(G)** Effects of *SIRT1* knockdown (*SIRT1si*) on *BMAL1*::LUC when all *ROR* isoforms are knocked down (*ROR(α-c)si*)**. (H)** Simulation results of *ROR* and *SIRT1* knockdown on *BMAL1* expression.

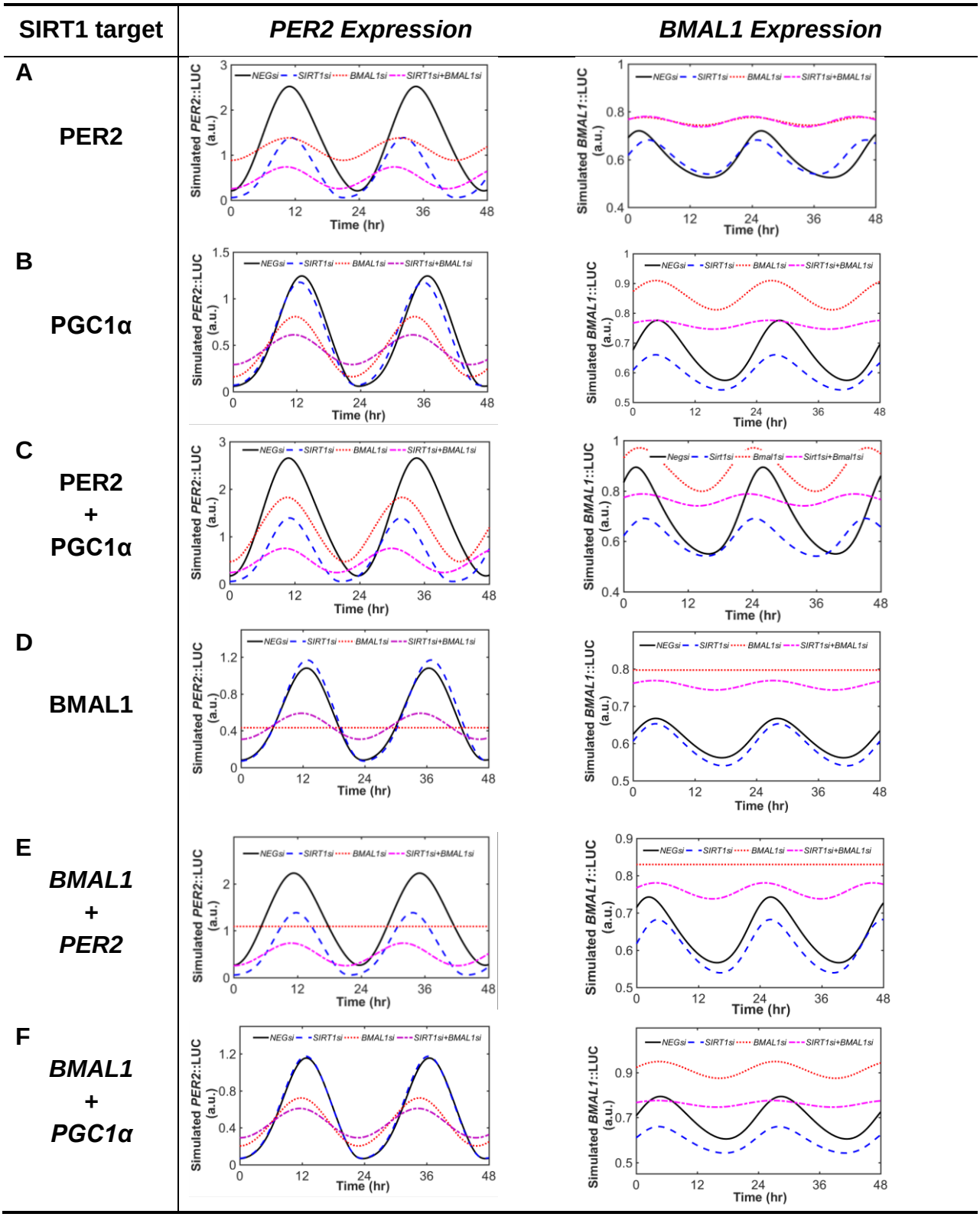

288 **Fig. S4. Related to Figure 2.** Simulation of the circadian effects of *SIRT1* and *BMAL1* knockdown on
289 *PER2/BMAL1* oscillations when SIRT1 regulates **(A)** only PER2, **(B)** only PGC1α, **(C)** both PER2 and
290 PGC1α, **(D)** only BMAL1, **(E)** both BMAL1 and PER2, or **(F)** both BMAL1 and PGC1α.

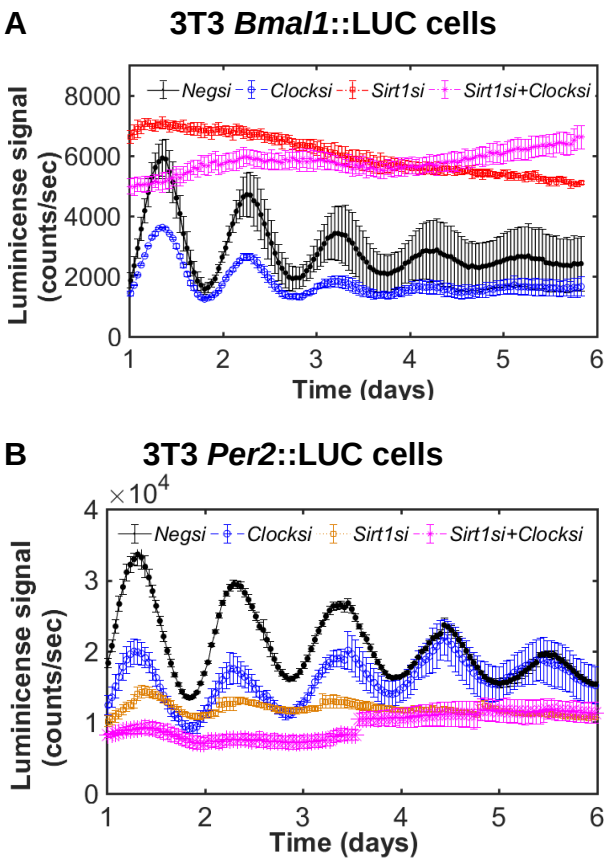

Fig. S5. Related to Figure 3. *SIRT1/CLOCK* knockdown effects on oscillations of the 3T3 cells in **(A)** *Bmal1*::LUC reporter lines and (**B**) *Per2*::LUC reporter lines. Data are represented as mean ± SEM.

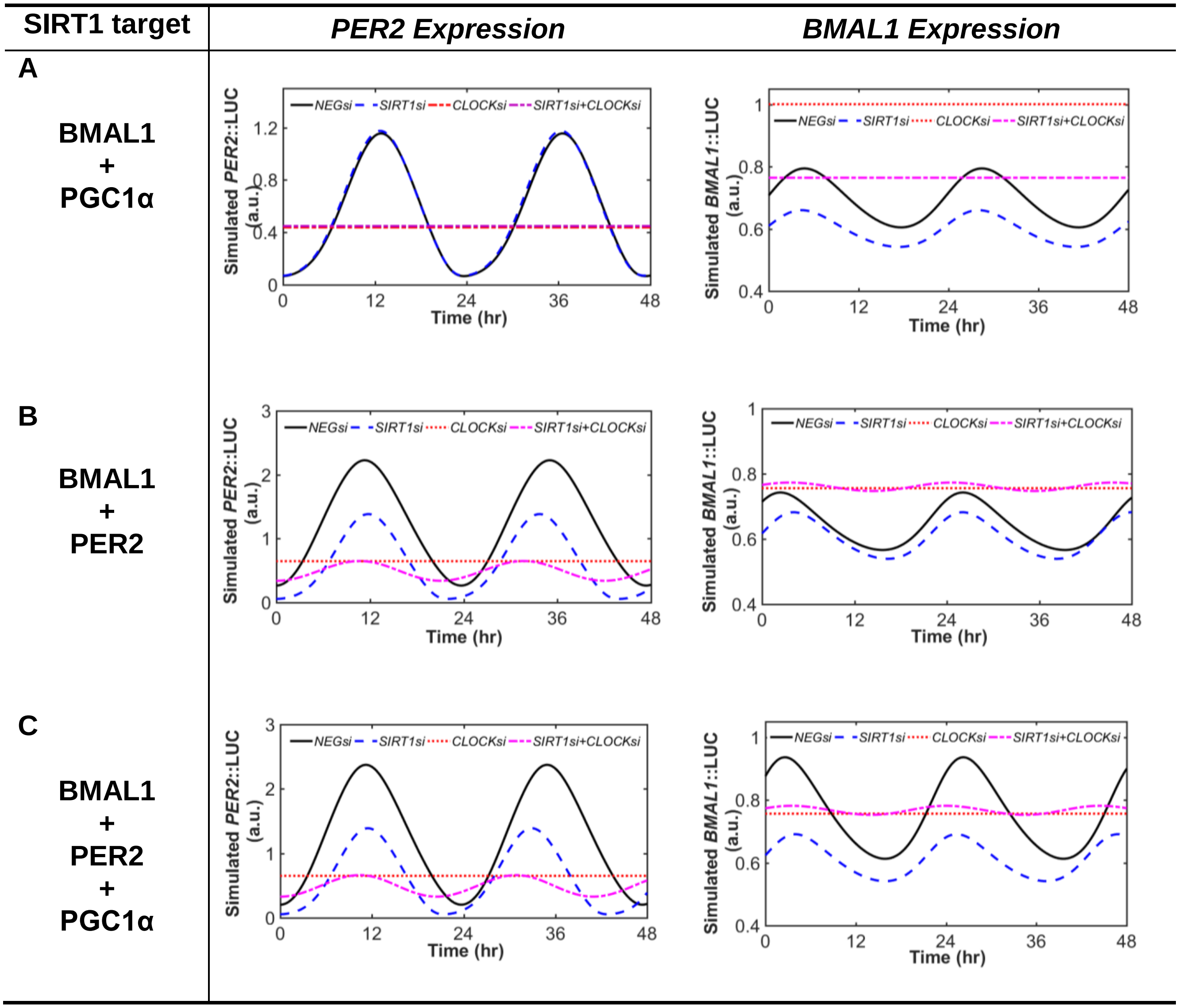

Fig. S6. Related to Figure 4. Simulation results of the circadian effects of *SIRT1* and *CLOCK* knockdown on *BMAL1*::LUC and *PER2*::LUC oscillations. Simulations are performed when considering SIRT1 regulates **(A)** BMAL1 and PGC1α, **(B)** BMAL1 and PER2, and **(C)** BMAL1, PER2 and PGC1α.

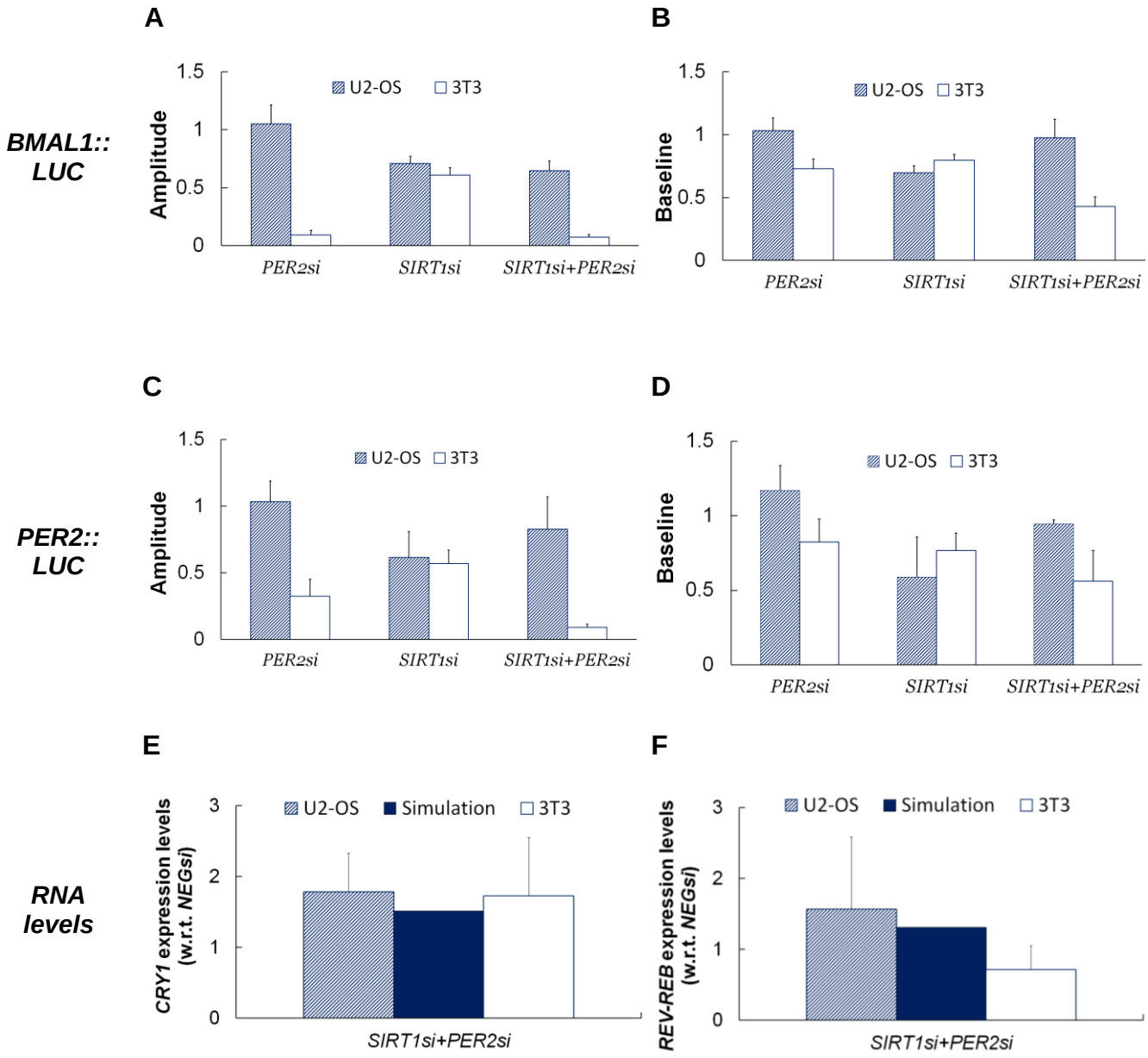

Fig. S7. Related to Figure 5. Circadian effect of *PER2* knockdown on *BMAL1* and *PER2* luciferase oscillations in both human U2-OS and mouse NIH 3T3 cell lines. **(A, B)** Experimentally measured amplitude and baseline of *BMAL1*::LUC oscillations from both U2-OS and 3T3 cells transfected with siRNAs targeting *PER2* (*PER2si*), *SIRT1* (*SIRT1si*) or both (*SIRT1si+PER2si*). Note the naming convention of U2-OS is used here for all data and simulation results. Amplitude and baseline of oscillations are normalized with respect to *NEGsi*. **(C, D)** Circadian amplitude and baseline of *PER2*::LUC oscillations measured under the same conditions as in (A, B). Comparison of model output and experimental RNA data for *CRY1* (E) and *REV-ERBα* (F) under *SIRT1si+PER2si* condition. Expression (RNA) levels are normalized with respect to control (*NEGsi*). Data are represented as mean ± SD. Note that gene names are represented in the uppercase italics naming convention (i.e. for genes of human origin) only for simplifying this figure's representation.

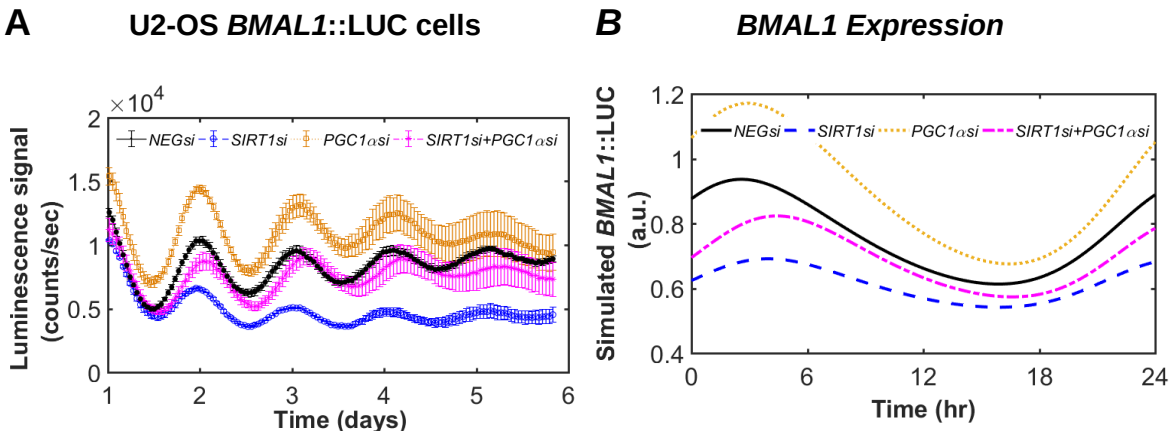

Fig. S8. Related to Figure 5. Circadian effect of *PGC1α* knockdown on *BMAL1* luciferase oscillations in human U2-OS cell line. **(A)** *SIRT1/PGC1α* dual knockdown effects on oscillations of U2-OS *BMAL1* reporter line. Data are represented as mean ± SEM. **(B)** *In silico* reproduction of the circadian effects of *SIRT1* and *PGC1α* knockdown on U2-OS *BMAL1* expression. Simulations are performed under conditions where SIRT1 does not deacetylate BMAL1 but deacetylates both PER2 and PGC1α. The model predicts the relevant *PGC1α* knockdown under the assumption that *PGC1αsi* induces an increase (i.e. 2-fold) in the active ROR complex association parameter ($k_{a,RP}$ – Table S7). In the absence of this assumption, model predictions are consistent with the experimental phenotype in 3T3 cells as shown in Figure's 5*E* and 5*F*.

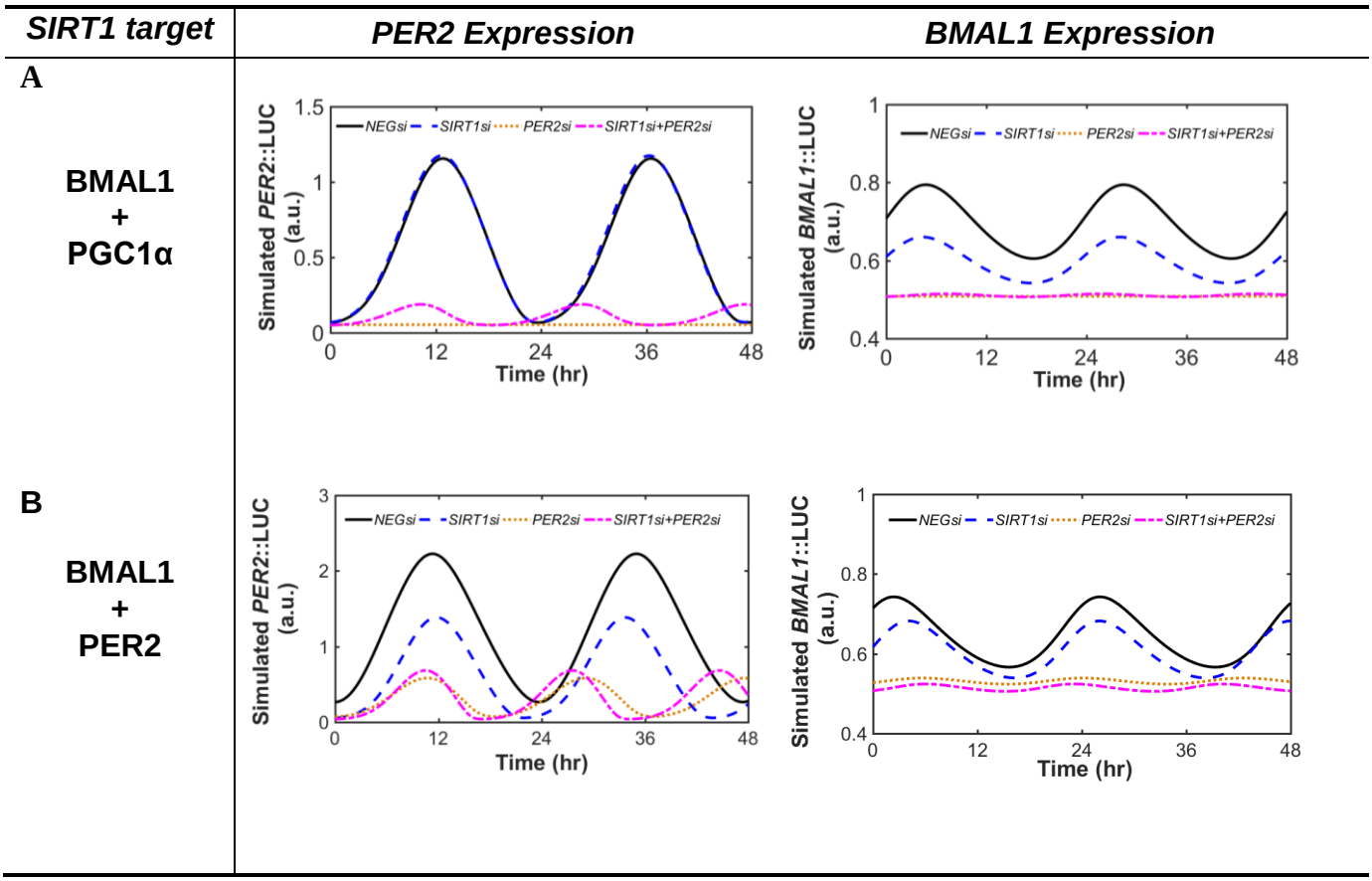

Fig. S9. Related to Figure 6. Simulation results of the circadian effects of *SIRT1* and *PER2* knockdown on *BMAL1*::LUC and *PER2*::LUC oscillations. Simulations are performed when considering SIRT1 regulates **(A)** BMAL1 and PGC1α and **(B)** BMAL1 and PER2.

Supplemental Tables

Table S1: Estimated values of parameters involved in the SIRT1-dependent regulation of BMAL1 and PER2 (model A)[§]

Parameter	Description of parameters	Set H1	Set H2
v_{0Per} (nM/hr)	Basal transcriptional rates of *PER*, *CRY* and *NAMPT* expression	0.007	0.002
v_{0Cry} (nM/hr)		0.414	0.163
v_{0Nampt} (nM/hr)		0.014	0.015
v_{sPer} (nM/hr)	Maximum transcriptional rates of *PER*, *CRY* and *NAMPT* mRNA	0.899	0.217
v_{sCry} (nM/hr)		0.443	0.131
v_{sNampt} (nM/hr)		0.390	0.212
K_{APer} (nM)	Michaelis constants for enhancement of *PER*, *CRY* and *NAMPT* expression by acetylated (active) BMAL1	1.864	0.713
K_{Acry} (nM)		0.934	0.581
K_{Anampt} (nM)		2.203	1.757
R_{Per} (nM)	Michaelis constants for inhibition of *PER*, *CRY* and *NAMPT* expression by acetylated (active) PER-CRY complex	0.921	0.059
R_{Cry} (nM)		1.148	0.044
R_{Nampt} (nM)		1.166	0.052
a	Hill coefficients for activation (a) and repression (r) of ccgs by acetylated BMAL1 and PER-CRY respectively	1	1
r		3	3
v_{dPer} (nM/hr)	Maximum degradation rates of *PER*, *CRY* and *NAMPT* mRNA	0.214	0.09
v_{dCry} (nM/hr)		0.452	0.024
v_{dNampt} (nM/hr)		0.284	0.228
K_{dPer} (nM)	Michaelis constants for degradation of *PER*, *CRY* and *NAMPT* mRNA	0.021	0.001
K_{dCry} (nM)		1.122	0.190
K_{dNampt} (nM)		0.569	1.937
k_{dn} (1/hr)	Nonspecific degradation rate constant	0.104	0.094
k_{sP} (1/hr)	Synthesis rate constants of PER, CRY and NAMPT proteins	1.269	0.253
k_{sC} (1/hr)		0.448	0.201
k_{sN} (1/hr)		0.849	0.160
$k_{a,PC}$ (1/hr)	Association and dissociation rate constants for the formation of the cytosolic PER-CRY complex	0.037	0.192
$k_{d,PC}$ (1/hr)		0.034	0.002
$k_{im,PC}$ (1/hr)	Rate constants for nuclear import of the cytosolic PER-CRY and BMAL1	0.367	0.233
$k_{im,B}$ (1/hr)		0.732	0.289
$k_{ex,PC}$ (1/hr)	Rate constants for exit of the nuclear proteins PER-CRY and BMAL1	0.020	0.046
$k_{ex,B}$ (1/hr)		1.117	0.738
v_{dPCC} (nM/hr)	Maximum degradation rates for the cytosolic and nuclear PER-CRY complex	0.068	0.033
v_{dPCN} (nM/hr)		0.039	0.183
K_{dPCC} (nM/hr)	Michaelis constants for degradation of the cytosolic and nuclear PER-CRY complex	1.252	0.082
K_{dPCN} (nM/hr)		1.024	0.196
v_{dP} (nM/hr)	Maximum degradation rates for the cytosolic proteins PER, CRY and NAMPT	0.493	4.8E-4
v_{dC} (nM/hr)		0.127	0.012
v_{dN} (nM/hr)		0.929	0.228
K_{dP} (nM)	Michaelis constants for degradation of the cytosolic proteins PER, CRY and NAMPT	1.551	0.019
K_{dC} (nM)		1.714	0.041
K_{dN} (nM)		1.549	2.052
k_{sB} (nM/hr)	Synthesis rate for constitutive BMAL1 expression	1.610	0.659
v_{dBC} (nM/hr)	Maximum degradation rate for the cytosolic protein BMAL1	0.458	0.148
K_{dBC} (nM)	Michaelis constant for degradation of the cytosolic protein BMAL1	0.302	0.036
v_{dBN} (nM/hr)	Maximum degradation rate for nuclear BMAL1	0.207	0.015

K_{dBN} (nM/hr)	Michaelis constant for degradation of nuclear BMAL1	1.838	1.788
v_{PAC} (nM/hr) v_{BAC} (nM/hr)	Maximum acetylation rates for nuclear proteins PER-CRY and BMAL1	0.604 0.997	0.258 0.293
v_{PDAC} (nM/hr) v_{BDAC} (nM/hr)	Maximum deacetylation rates for nuclear PER-CRY and BMAL1	0.121 0.659	0.248 0.275
K_{PAC} (nM) K_{BAC} (nM)	Michaelis constants for protein acetylation of PER-CRY and BMAL1	0.145 3.488	0.028 0.169
K_{PDAC} (nM) K_{BDAC} (nM)	Michaelis constants for protein deacetylation of PER-CRY and BMAL1 by NAD	1.934 3.221	0.012 0.035
s_n (nM/hr)	Synthesis rate constant of cellular NAD levels	0.524	0.126
v_{dNAD} (nM/hr)	Maximum degradation rate for intracellular NAD	0.284	0.200
K_{dNAD} (nM)	Michaelis constant for NAD degradation	1.530	1.150

[§]Rate parameters of sets H1 and H2 are scaled giving rise to wild type circadian oscillations (period ~23.7hr). While parameter set H1 reproduces the increased amplitude phenotype due to lack of *SIRT1* as shown by (4), parameter set H2 reproduces the reduced amplitude phenotype as reported by (13).

Table S2: Model parameters used to simulate siRNA experiments[†]

siRNA	Parameter symbol	Control value	*siRNA* value
BMAL1si	k_{sB}	1.073	0.429
PER2si	v_{dPer2}	0.302	0.423
	v_{dCry}	0.285	0.214
	v_{dREV}	0.361	0.271
CLOCKsi	v_{BAC}	0.317	0.152
RORsi	v_{mRor}	0.309	0.463
SIRT1si	s_n	0.351	0.0187
PGC1αsi	v_{dpgc}	0.388	0.775

[†]Note the control values for all model parameters are summarized in **Table S7**.

Table S3: siRNA and Primers used for QPCR (experimental section)

siRNA used	***Catalog#***	***Company***	***Catalog#***	***Company***
Gene	**Mouse**		**Human**	
BMAL1	Flexitube GS11865	Qiagen	see (15) for Sequence	
CLOCK	Flexitube GS1275	Qiagen	see (15) for Sequence	
RORA	Flexitube GS19883	Qiagen	see (15) for Sequence	
RORB	Flexitube GS22599	Qiagen	see (15) for Sequence	
RORC	Flexitube GS19885	Qiagen	see (15) for Sequence	
PER2	Flexitube GS18627	Qiagen	Flexitube Human GS8864	Qiagen
SIRT1	Flexitube GS93759	Qiagen	Flexitube GS23411 Human	Qiagen

Primers used for QPCR	***Catalog#***	***Company***	***Catalog#***	***Company***
Gene	Mouse		Human	
BMAL1	Mm00500226_m1	ABI/Lifetechnologies	Hs00154147_m1	ABI/Lifetechnologies
CLOCK	Mm00455950_m1	ABI/Lifetechnologies	Hs00231857_m1	ABI/Lifetechnologies
CRY1	Mm00514392_m1	ABI/Lifetechnologies	Hs00172734_m1	ABI/Lifetechnologies
CRY2	Mm00546062_m1	ABI/Lifetechnologies	Hs00323654_m1	ABI/Lifetechnologies
DBP	Mm00497539_m1	ABI/Lifetechnologies	Hs00609747_m1	ABI/Lifetechnologies
NR1D1	Mm00520708_m1	ABI/Lifetechnologies	Hs00253876_m1	ABI/Lifetechnologies
NR1D2	Mm00441730_m1	ABI/Lifetechnologies	Hs00233309_m1	ABI/Lifetechnologies
PER1	Mm00561813_m1	ABI/Lifetechnologies	Hs00242988_m1	ABI/Lifetechnologies
PER2	Mm00478113_m1	ABI/Lifetechnologies	Hs00256143_m1	ABI/Lifetechnologies
PGC1α	Mm001208835_m1	ABI/Lifetechnologies	Hs01016719_m1*	ABI/Lifetechnologies
RORA	Mm.PT.58.32675621	IDT	Hs00536545_m1	ABI/Lifetechnologies
RORB	Mm.PT.58.9944191	IDT	Hs00199445_m1	ABI/Lifetechnologies
RORC	Mm.PT.58.8455991	IDT	Hs01076112_m1	ABI/Lifetechnologies

Note that gene names are represented in the uppercase italics naming convention (i.e. for genes of human origin) only for simplifying this table's representation.

Table S4: Data/phenotypes used for the development and validation of model A and model B

Model A: Modeling the SIRT1-dependent regulation of BMAL1 and PER2	
Model development (cost function)	**PER-CRY negative feedback loop: essential for generating oscillations** The transcriptional/translational PER-CRY loop gives rise to oscillations, while the metabolic feedback loop regulates the circadian amplitude
	Phase optimization for mRNA of clock controlled genes (ccgs) Phases for mRNA of clock controlled genes (i.e., *PER, CRY, NAMPT*) are optimized including also the phases of metabolic signaling components (NAMPT, NAD^+) **Amplitude optimization:** Although the model is mostly calibrated using phase data, relevant amplitudes for the NAD signaling components are considered but they are not weighted highly in the cost function
	Metabolic null mutation (i.e. $SIRT1^{-/-}$): Negligible period variance (±1h) while capturing significant amplitude sensitivity Under conditions of metabolic null mutation, the cost function is customized such that the amplitude of CCGs significantly varies with respect to WT by ±20%. The directionality of the amplitude (up- or down-regulation) is optimized based on the following experimental studies: **(**4**):** Increased circadian amplitude (*$SIRT1^{-/-}$*) (*parameter set H1*) **(**13**):** Reduced circadian amplitude (*$SIRT1^{-/-}$*) (*parameter set H2*)
Model validation (literature data)	**PER protein: rate-limiting component of PER-CRY negative limb** As the rate-limiting factor, the protein PER dictates the rhythmic formation of PER-CRY repressor
	Predict phase relationships of CCGs and NAD^+ signaling components We test if the simulated phase of PER protein (rate-limiting component of negative limb) is ~4-8h later vs. its respective mRNA dynamics Further, the predicted phase of acetylated BMAL1 (not optimized) is compared with that of its regulator (NAD)
	$BMAL1^{-/-}$: Predict no oscillations & reduced constitutive expression of ccgs BMAL1 is an essential clock component of the positive limb (activator) and therefore cell extracts deficient in *BMAL1* display arrhythmias while NAMPT or NAD levels are reduced compared to the WT
	$CRY^{-/-}$: Predict no oscillations & increased constitutive of ccgs CRY1/CRY2 are essential components (repressors) of the negative limb of the core clock machinery. Double KO of *CRY1/CRY2* accounts for loss of rhythmicity and increased *NAMPT* expression and/or NAD levels

Model B: Modeling the SIRT1-dependent regulation of BMAL1, PER2 and PGC1α	
Model development (cost function)	**PER/CRY negative loop: essential for generating oscillations** The transcriptional PER/CRY loop gives rise to sustained oscillations while the core clock continues to oscillate in the absence of *REVERB* or *ROR* genes **REV-ERB negative loop: not essential for oscillations but crucial for Bmal1 rhythmicity**
	Phase optimization The phases for mRNA of clock genes (i.e. *PER, CRY, NAMPT*) are optimized including also the phases of NAMPT protein and NAD metabolite. While the phase difference between *REV-ERB* and *ROR* mRNA is not optimized, the anti-phase relationship between *BMAL1* and *PER* mRNA is considered in the cost function **Amplitude optimization:** Although the model is mostly calibrated using phase data,

	relevant amplitudes for the metabolic NAD loop and ROR/REVERB module are considered but they are not weighted highly in the cost function
	Metabolic null mutation (i.e. *SIRT1*$^{-/-}$): Reduced baseline/amplitude for RORE genes In the absence of *SIRT1* expression, the cost function is customized such that the mRNA baseline of RORE genes (i.e. *ROR* and *BMAL1*) are significantly reduced when compared to WT **Loss-of-function mutation for *BMAL1* using RNAi experiment (Bmal1si): Increased baseline of *BMAL11* promoter but reduced amplitude** Given the opposing activities of ROR and REV-ERB proteins at the *BMAL1* promoter, model parameters are set to consider REV-ERB as the dominant force within the ROR/REV-ERB loop. This in turn allows the model to capture the increased baseline of *BMAL1* expression in the Bmal1si mutant due to reduction in *REV-ERB* expression.
Model validation (main RNAi experiments)	**Loss-of-function mutation for *SIRT1* and *BMAL1* (Sirt1+Bmal1si)** *SIRT1* knockdown lowers baseline and amplitude of circadian gene expression when *BMAL1* is also knocked down
	Loss-of-function mutation for *CLOCK* (Clocksi) *CLOCK* knockdown increases the baseline of *BMAL1* mRNA but lowers the amplitude similar to the Bmal1si mutant **Loss-of-function mutation for *SIRT1* and *CLOCK* (Sirt1si+Clocksi)** Similar responses to Bmal1si+Sirt1si **Loss-of-function mutation for *SIRT1* and *PER2* (Sirt1si+Per2si)** The dual knockdown of *PER2* and *SIRT1* compromises the amplitude of *PER2* promoter gene expression.

Table S5: Experimental and simulated phases[†]

Model components	Experimental phase, hr (peak expression)	Simulated phase, hr (set H1)	Simulated phase, hr (set H2)
PER expression	Per1: [10-16] Per2: [14-18]	~14	~14
CRY expression	Cry1: [14-18] Cry2: [8-12]	~14	~14
NAMPT expression	~14	~13	~13
NAMPT (protein)	[14-22]	~15	~17
NAD^+ (cofactor)	[14-22]	~18	~20

[†]Experimental phases are compiled from literature evidence (6, 4, 16-20,) using peripheral (metabolically active) tissues including data derived from liver. The experimental phase range for *PER* and *CRY* mRNA is derived from the studies (6, 18-20) and it is defined as the average circadian time (CT) at peak expression. For example, *PER* mRNA levels peak on average at CT13 and fall at CT0 during the beginning of the subjective day (18). According to the study (16) the gene transcript of *NAMPT* also peaks early in the evening (approximately at CT14) while its protein (NAMPT) peaks later together with the circadian NAD+ levels which are in phase with the rhythmic SIRT1 activity.

Table S6: Averaged U2-OS and 3T3 QPCR data for all knockdowns[†]

		U2-OS	3T3	U2-OS	3T3
BMAL 1		***BMAL1si***		***SIRT1si+BMAL1si***	
	Mean	0.403	0.521	0.420	0.483
	SD	0.169	0.137	0.141	0.102
	N	11	8	10	8
SIRT1	Mean			0.195	0.206
	SD			0.063	0.046
	N			13	12
CLOCK		***CLOCKsi***		***SIRT1si+CLOCKsi***	
	Mean	0.481	0.261	0.262	0.232
	SD	0.340	0.094	0.096	0.08
	N	10	8	10	8
SIRT1	Mean			0.163	0.182
	SD			0.042	0.06
	N			10	8
PER2		***PER2si***		***SIRT1si+PER2si***	
	Mean	0.437	0.466	0.336	0.290
	SD	0.224	0.167	0.119	0.153
	N	9	8	9	8
SIRT1	Mean			0.186	0.215
	SD			0.058	0.077
	N			9	8
PGC1α		***PGC1αsi***		***SIRT1si+PGC1αsi***	
	Mean	0.440	0.226	0.518	0.302
	SD	0.190	0.092	0.272	0.087
	n	6	8	4	7
SIRT1	Mean			0.518	0.302
	SD			0.272	0.087
	N			4	7
RORa		***ROR(α-c)si***		***SIRT1si+ROR(α-c)si***	
	Mean	0.756	0.131	1.267	0.192
	SD	0.734	0.025	1.501	0.161
	n	6	9	6	9
RORb	Mean	0.272	U.D.	1.842	U.D.
	SD	0.160	U.D.	2.295	U.D.
	N	5	>3	6	>3
RORc	Mean	0.272	U.D.	0.296	U.D.
	SD	0.156	U.D.	0.197	U.D.
	N	4	>3	5	>3
SIRT1				0.191	0.175
				0.043	0.046
				7	9
SIRT1		***SIRT1si***			
	Mean	0.195	0.206		
	SD	0.063	0.046		
	N	13	12		

[†]All gene expressions are fold change over control cells treated with scrambled siRNA. SD = Standard deviation. U.D = Undetermined. Note that gene names are represented in the uppercase italics naming convention (i.e. for genes of human origin) only for simplifying this table's representation.

Table S7: Estimated values of parameters involved in the development of the extended circadian model (model B)

Parameter	Description of parameters	Value
$v_{0Per(1/2)}$ (nM/hr)	Basal transcriptional rates of *PER(1/2)*, *CRY*, *NAMPT*, *REVERB*, *ROR* and *BMAL1* expression	0.026
v_{0Cry} (nM/hr)		0.270
v_{0Nampt} (nM/hr)		0.251
v_{0Rev} (nM/hr)		0.040
v_{0Ror} (nM/hr)		0.178
v_{0B} (nM/hr)		0.405
$v_{sPer(1/2)}$ (nM/hr)	Maximum transcriptional rates of *PER(1/2)*, *CRY*, *NAMPT*, *REVERB*, *ROR* and *BMAL1* expression	1.144
v_{sCry} (nM/hr)		0.072
v_{sNampt} (nM/hr)		1.485
v_{sRev} (nM/hr)		0.901
v_{s1Ror} (nM/hr)		0.744
v_{s2Ror} (nM/hr)		0.052
v_{sB} (nM/hr)		0.417
$K_{APer(1/2)}$ (nM)	Michaelis constants for enhancement of *PER(1/2)*, *CRY*, *NAMPT*, *REVERB* and *ROR* expression by acetylated (active) BMAL1	1.150
K_{ACry} (nM)		0.291
K_{ANampt} (nM)		1.844
K_{ARev} (nM)		4.755
K_{A1Ror} (nM)		2.483
$R_{Per(1/2)}$ (nM)	Michaelis constants for inhibition of *PER(1/2)*, *CRY*, *NAMPT*, *REVERB* Michaelis constants for inhibition of *PER(1/2)*, *CRY*, *NAMPT*, *REVERB* and *ROR* expression by PER1-CRY complex and *ROR* expression by PER1-CRY complex	0.960
R_{Cry} (nM)		0.675
R_{Nampt} (nM)		1.074
R_{Rev} (nM)		1.506
R_{1ror} (nM)		0.970
$R'_{Per(1/2)}$ (nM)	Michaelis constants for inhibition of *PER(1/2)*, *CRY*, *NAMPT*, *REVERB* and *ROR* expression by acetylated $PER2^{AC}$-CRY complex	0.160
R'_{Cry} (nM)		0.112
R'_{Nampt} (nM)		0.179
R'_{Rev}		0.251
R'_{1Ror}		0.162
K_{AB} (nM)	Michaelis constants for enhancement of *BMAL1* and *ROR* expression by active ROR^*	1.468
K_{A2Ror} (nM)		7.244
R_B	Michaelis constants for inhibition of *BMAL1* and *ROR* expression by REV-ERB	0.0159
R_{2Ror}		2.55
a	Hill coefficients for activation (a) and repression (r) of ccgs by acetylated BMAL1 and PER-CRY respectively	2
r		4
b	Hill coefficients for activation (b) and repression (c) of RORE by active ROR^* and REV-ERB respectively	2
c		3
$v_{dPer(1/2)}$ (nM/hr)	Maximum degradation rates of *PER(1/2)*, *CRY*, *NAMPT*, *REVERB*, *ROR* and *BMAL1* expression	0.302
v_{dCry} (nM/hr)		0.285
v_{dNampt} (nM/hr)		0.594
v_{dRev} (nM/hr)		0.361
v_{dRor} (nM/hr)		0.309
v_{dB} (nM/hr)		0.473
$K_{dPer(1/2)}$ (nM)	Michaelis constants for degradation of *PER(1/2)*, *CRY*	0.047
K_{dCry} (nM)		0.371
K_{dNampt} (nM)	Michaelis constants for degradation of *NAMPT*, *REVERB*, *ROR*	0.99
K_{dRev} (nM)		0.691

K_{dRor} (nM)	and *BMAL1* mRNA	3.659
K_{dB} (nM)		0.135
k_{dn} (1/hr)	Nonspecific degradation rate constant	0.077
k_{sP1} (1/hr)	Synthesis rate constants of PER(1/2), CRY , NAMPT, REV-ERB, ROR and BMAL1 proteins	1.009
k_{sP2} (1/hr)		0.727
k_{sC} (1/hr)		1.407
k_{sN} (1/hr)		1.295
k_{sREV} (1/hr)		0.167
k_{sROR} (1/hr)		0.320
k_{sB} (1/hr)		1.073
$k_{a,P1C}$ (1/hr)	Association and dissociation rate constants for the formation of PER1-CRY and PER2-CRY complex	0.006
$k_{d,P1C}$ (1/hr)		0.006
$k_{a,P2C}$ (1/hr)		0.088
$k_{d,P2C}$ (1/hr)		0.192
$k_{im,B}$ (1/hr)	Rate constants for nuclear import and export of the cytosolic BMAL1	0.783
$k_{ex,B}$ (1/hr)		0.617
v_{dP1C} (nM/hr)	Maximum degradation rates for PER1-CRY and PER2-CRY complexes	0.069
v_{dP2C} (nM/hr)		0.243
K_{dP1C} (nM/hr)	Michaelis constants for degradation of PER1-CRY and PER2-CRY complexes	0.575
K_{dP2C} (nM/hr)		0.575
v_{dP1} (nM/hr)	Maximum degradation rates for the proteins PER(1/2), CRY, NAMPT, REV-ERB, ROR and BMAL1	1.285
v_{dP2} (nM/hr)		0.698
v_{dC} (nM/hr)		0.265
v_{dN} (nM/hr)		1.211
v_{dREV} (nM/hr)		0.387
v_{dROR} (nM/hr)		0.179
v_{dBc} (nM/hr)		0.104
K_{dP} (nM)	Michaelis constants for degradation of the proteins PER(1/2), CRY, NAMPT, REV-ERB, ROR and BMAL1	0.478
K_{dC} (nM)		1.247
K_{dN} (nM)		0.917
K_{dREV} (nM)		0.796
K_{dROR} (nM)		4.893
K_{dBc} (nM)		0.135
v_{dBN} (nM/hr)	Maximum degradation rate for nuclear BMAL1	2.212
K_{dBN} (nM/hr)	Michaelis constant for degradation of nuclear BMAL1	3.392
v_{PAC} (nM/hr)	Maximum acetylation rates for proteins PER2-CRY and BMAL1	0.254
v_{BAC} (nM/hr)		0.318
v_{PDAC} (nM/hr)	Maximum deacetylation rates for PER2-CRY and BMAL1	0.233
v_{BDAC} (nM/hr)		0.0024
K_{PAC} (nM)	Michaelis constants for protein acetylation of PER2-CRY and BMAL1	8.149
K_{BAC} (nM)		0.497
K_{PDAC} (nM)	Michaelis constants for protein deacetylation of PER2-CRY and BMAL1 by NAD	4.998
K_{BDAC} (nM)		4.016
s_n (nM/hr)	Synthesis rate constant of cellular NAD levels	0.351
v_{dNAD} (nM/hr)	Maximum degradation rate for intracellular NAD	0.881
K_{dNAD} (nM)	Michaelis constant for NAD degradation	1.650
v_{0pgc} (nM)	Basal activation rate of PGC1α	0.046

v_{spgc} (nM)	Maximum activation rate by NAD	0.0142
K_{Apgc} (nM)	Michaelis activation constant for PGC1α	7.578
v_{dpgc} (nM)	Maximum degradation rate for PGC1α activity	0.388
K_{dpgc} (nM)	Michaelis constant for degradation of active PGC1α	3.299
$k_{a,RP}$ (1/hr)	Association and dissociation rate constants for the formation of active ROR* complex	0.621
$k_{d,RP}$ (1/hr)		0.329

388

389

References

1. Price TS, Baggs JE, Curtis AM, Fitzgerald GA, & Hogenesch JB (2008) WAVECLOCK: wavelet analysis of circadian oscillation. Bioinformatics 24(23):2794-2795.
2. Yamamoto Y, Yagita K, & Okamura H (2005) Role of cyclic mPer2 expression in the mammalian cellular clock. Mol Cell Biol 25(5):1912-1921.
3. Liu AC, et al. (2008) Redundant function of REV-ERBalpha and beta and non-essential role for Bmal1 cycling in transcriptional regulation of intracellular circadian rhythms. PLoS Genet 4(2):e1000023.
4. Nakahata Y, et al. (2008) The NAD+-dependent deacetylase SIRT1 modulates CLOCK-mediated chromatin remodeling and circadian control. Cell 134(2):329-340.
5. Yagita K, Tamanini F, van Der Horst GT, & Okamura H (2001) Molecular mechanisms of the biological clock in cultured fibroblasts. Science 292(5515):278-281.
6. Lee C, Etchegaray JP, Cagampang FRA, Loudon ASI, & Reppert SM (2001) Posttranslational mechanisms regulate the mammalian circadian clock. Cell 107(7):855-867.
7. Bellet MM & Sassone-Corsi P (2010) Mammalian circadian clock and metabolism - the epigenetic link. J Cell Sci 123(Pt 22):3837-3848.
8. Becker-Weimann S, Wolf J, Herzel H, & Kramer A (2004) Modeling feedback loops of the mammalian circadian oscillator. Biophys J 87(5):3023-3034.
9. Ueda HR, Hagiwara M, & Kitano H (2001) Robust oscillations within the interlocked feedback model of Drosophila circadian rhythm. J Theor Biol 210(4):401-406.
10. Bernard S, Gonze D, Cajavec B, Herzel H, & Kramer A (2007) Synchronization-induced rhythmicity of circadian oscillators in the suprachiasmatic nucleus. PLoS Comput Biol 3(4):e68.
11. Chen R, et al. (2009) Rhythmic PER abundance defines a critical nodal point for negative feedback within the circadian clock mechanism. Mol Cell 36(3):417-430.
12. D'Alessandro M, et al. (2015) A tunable artificial circadian clock in clock-defective mice. Nat Commun 6:8587.
13. Asher G, et al. (2008) SIRT1 regulates circadian clock gene expression through PER2 deacetylation. Cell 134(2):317-328.
14. Liu C, Li S, Liu T, Borjigin J, & Lin JD (2007) Transcriptional coactivator PGC-1alpha integrates the mammalian clock and energy metabolism. Nature 447(7143):477-481.
15. Baggs JE, et al. (2009) Network features of the mammalian circadian clock. PLoS Biol 7(3):e52.
16. Ramsey KM, et al. (2009) Circadian Clock Feedback Cycle Through NAMPT-Mediated NAD(+) Biosynthesis. Science 324(5927):651-654.
17. Naimi M, Arous C, & Van Obberghen E (2010) Energetic cell sensors: a key to metabolic homeostasis. Trends Endocrinol Metab 21(2):75-82.
18. Yamamoto T, et al. (2004) Transcriptional oscillation of canonical clock genes in mouse peripheral tissues. BMC Mol Biol 5:18.
19. Ueda HR, et al. (2002) A transcription factor response element for gene expression during circadian night. Nature 418(6897):534-539.
20. Ripperger JA, Jud C, & Albrecht U (2011) The daily rhythm of mice. FEBS Lett 585(10):1384-1392
21. Gutenkunst RN, et al. (2007) Universally sloppy parameter sensitivities in systems biology models. PLoS Comput Biol 3(10):1871-1878.
22. Belden WJ & Dunlap JC (2008) SIRT1 is a circadian deacetylase for core clock components. Cell 134(2):212-214.
23. Fuller PM, Lu J, & Saper CB (2008) Differential rescue of light- and food-entrainable circadian rhythms. Science 320(5879):1074-1077.